

# A Quantum-Inspired Attention Network with Orthogonal Polynomials for Medical Image Classification

Senthilkumar Jagatheesan<sup>1,\*</sup>, Devendranath K<sup>2,\*\*</sup>, and N Sameer Kumar<sup>3,\*\*\*</sup>

<sup>1</sup>Department of CSE, Vel Tech Rangarajan Dr.Sagunthala R&D Institute of Science and Technology, Chennai, Tamil Nadu, India.

<sup>2,3</sup>Department of CSE(AI&ML), Vel Tech Rangarajan Dr.Sagunthala R&D Institute of Science and Technology, Chennai, Tamil Nadu, India.

**Abstract.** In this research, an Orthogonal Polynomials Transformation and Quantum Inspired Attention Network (QIAN) based medical image classification framework called QuAntNet is presented. It integrates low level image features are automatically extracted from brain MRI images with expert level clinical insights to identify diagnosis precise classes. The proposed method extracts fusion edge, texture and deep level features from the image based on OPT and Convolutional Neural Network techniques. The extracted classical features are submitted to quantum-inspired attention network mechanism for analyzing intricate relationships between different discriminative image features. The QuAntNet is validated on reputed brain MRI datasets namely BraTS2020 and Figshare, which includes different classes of brain tumors. Experiment conducted on BraTS2020 dataset, the QuAntNet method establishes overall accuracy upto 98.7%, sensitivity upto 98.2%, specificity upto 99.0% and F1-score of 98.4%. Also, when validated on Figshare, it produces accuracy of 99.3%, sensitivity of 98.9%, specificity of 99.6% and F1-score of 99.1%. Experimental outcomes clearly validates that there is significant enhancement in classification accuracy incorporating fusion edge, texture and deep features and QIAN methods enhances the classification performance in the QuAntNet framework.

**Index terms:** Brain tumor diagnosis, Low level features, Orthogonal polynomials transformation, Quantum feature fusion, Quantum-inspired attention networks, Quantum support vector machine.

## 1 Introduction

Magnetic Resonance Imaging(MRI) technique is an important aspect in the diagnosis and prognosis of the neurological disorders like glioma, meningioma, alzheimer disease and multiple sclerosis. The problem of automated MRI brain image classification has emerged as a critical research trend because of the growing clinical load, inter-observer variability, and the necessity of early and accurate diagnosis[1]. Traditional machine learning methods usually use features extracted by hand, while deep learning systems like CNNs create hierarchical representations of the image directly from raw image data. There are many examples of the

\*e-mail: adhityaresearch@hotmail.com

\*\*e-mail: devendranathkapa@gmail.com

\*\*\*e-mail: kumarsameer96933@gmail.com

high performance of CNN based models for the medical image analysis domain; however, them solely relying on either handcrafted edge and texture descriptors or deep learnt convolutional features for discrimination could limit their discriminative ability[3]. Additionally, conventional preprocessing methods often fail to capture edge structures that are fine grain in nature and texture variations that are small and therefore important in the accurate delineation and classification of tumors. Therefore, a mathematically rigorous feature enhancement strategy that is able to be integrated into a deep learning model is needed to make the representations obtained from the model better, resulting in a more accurate diagnosis[11].

Orthogonal Polynomials Transformation (OPT) have also gained popularity in recent times in image processing for their efficiency. The orthogonal property allows efficient representation of spatial information such as edges and textures in medical images. The orthogonal moments and projections have shown promising results in edge detection, pattern recognition, and biomedical image processing tasks [14]. The orthogonal polynomials transformation of MRI images can highlight tumor-specific information, and these transformation are very appropriate for highlighting tumor texture features.

QuAntNet framework proposed will use the combined strength of orthogonal polynomials based edge and texture features and CNN based deep features representation to improve the classification of brain tumors in MRIs. Specifically, the orthogonal polynomials transformation find a number of compact and non-redundant edge and texture descriptors, which will serve to emphasise the continuity of edge, sharpness of edges, and variations in fine structure from MRI images of the tumor region; meanwhile, the CNN modules will learn hierarchical semantic and morphological representations of the images. These three types of features, edge, texture and deep, will then be fused using a quantum inspired integration methodology followed by a quantum inspired attention mechanism for modelling higher order relationships before generating a classification[10]. Experimental evaluation demonstrates the superior performance exhibited by the QuAntNet architecture across datasets in classifying tumors in MRIs[4][9][12].

The remainder of this paper is structured as follows. Section II will present the background work that lays out the theoretical foundation of quantum-inspired feature extraction, orthogonal polynomial transformation, and qubit-based feature encoding. Section III will discuss some related works on brain tumor detection and classification based on texture and deep feature extraction methods. Section IV presents the QuAntNet based brain image classification framework. Section V discusses experimental setup followed by its results and a comparative analysis on BraTS 2020 and Figshare brain tumor MRI datasets highlighting accuracy, sensitivity, specificity, and F1- score is detailed in. Finally, Section VI concludes the paper by summarizing the main findings and outlining potential directions for future research and clinical deployment.

## 2 Background Works

### 2.1 Orthogonal Polynomials Model

A 2D image can be modeled as the linear output of an imaging system applied to an input object can be described using a separable blurring point spread operator within a Cartesian coordinate framework. In this approach, the captured image  $I$  is generated by combining multiple point source impulses, where each impulse is scaled according to the corresponding function value representing the object  $f$ .

The point spread function  $M(x, y)$  is modeled as a real-valued function defined on the spatial domain  $(x, y) \in X \times Y$ , where  $X$  and  $Y$  denote ordered sets of real spatial coordinates.

In the case of an  $n \times n$  grayscale image, the row coordinate set  $X$  becomes discrete and bounded. For practical representation, these coordinates can be indexed in a finite manner.

$$X = \{0, 1, \dots, n - 1\}.$$

Under the discrete framework,  $M(x, y)$  is represented as an ordered set of function values indexed by the sampled coordinate locations as in equation (1):

$$M(i, t) = u_i(t), \quad i, t = 0, 1, \dots, n - 1 \quad (1)$$

The 2D transform is given by equation (2):

$$\beta'(\zeta, \eta) = \int_X \int_Y M(\zeta, x)M(\eta, y)I(x, y) dx dy \quad (2)$$

where  $\beta'$  represents the transform coefficients.

In discrete form, this becomes as shown in equation (3):

$$|\beta'_{ij}| = (|M| \otimes |M|)'|I| \quad (3)$$

where  $|M|$  represents the *matrix of orthogonal basis functions*, and  $\otimes$  denotes the *outer product*.

The matrix  $|M|$  is constructed using orthogonal polynomials  $u_0(t), u_1(t), \dots, u_{n-1}(t)$ , as illustrated in equation (4):

$$|M| = \begin{bmatrix} u_0(t_1) & u_1(t_1) & \cdots & u_{n-1}(t_1) \\ u_0(t_2) & u_1(t_2) & \cdots & u_{n-1}(t_2) \\ \vdots & \vdots & \ddots & \vdots \\ u_0(t_n) & u_1(t_n) & \cdots & u_{n-1}(t_n) \end{bmatrix} \quad (4)$$

The orthogonal polynomials are generated recursively as represented in equation (5) and equation (6):

$$u_{i+1}(t) = (t - \mu)u_i(t) - b_i(n)u_{i-1}(t), \quad u_1(t) = t - \mu, \quad u_0(t) = 1 \quad (5)$$

where

$$b_i(n) = \frac{i^2(n^2 - i^2)}{4(4i^2 - 1)}, \quad \mu = \frac{1}{n} \sum_{t=1}^n t = \frac{n+1}{2} \quad (6)$$

The recursive formulations guarantee the orthogonality of the polynomial set, enabling them to serve as valid basis functions for image transform coding. Using these polynomials, point-spread operators of different sizes can be generated for  $n \geq 2$  through suitable parameter selection. For efficient practical implementation, the resulting operator matrices are scaled so that all elements assume integer values.

## 2.2 The Orthogonal Polynomials Basis

For ease of computation, the finite Cartesian coordinate sets  $X$  and  $Y$  are indexed in the form  $\{1, 2, 3, \dots, n\}$ . The point-spread operator responsible for the linear orthogonal transformation used in image coding is expressed as  $|M| \otimes |M|$ , where  $|M|$  is obtained and normalized based on the previously defined formulations in equation (7).

$$|Z| = |H^T||I| = (|M^T||M|)^{-1/2}|M^T||I| = (|M^T||M|)^{-1/2}|\beta'| \quad (7)$$

Here,  $|H\rangle$  is a *unitary operator*, ensuring energy preservation in equation (8):

$$|H\rangle = (|M\rangle \otimes |M\rangle) \times ((|M\rangle \otimes |M\rangle)^T (|M\rangle \otimes |M\rangle))^{-1/2} \quad (8)$$

Thus, the image reconstruction becomes as shown in equation (9):

$$|I\rangle = |H\rangle|Z\rangle = |M\rangle|\beta\rangle = \sum_{i=0}^{n-1} \sum_{j=0}^{n-1} \beta_{ij}|O_{ij}\rangle \quad (9)$$

Bessel's equality confirms that the orthogonal transform is complete as depicted in equation (10):

$$\langle |I\rangle, |I\rangle \rangle = \langle |Z\rangle, |Z\rangle \rangle \quad (\text{Bessel's Equality}) \quad (10)$$

or equivalently as represented in equation (11),

$$\sum_{i=0}^{n-1} \sum_{j=0}^{n-1} I_{ij}^2 = \sum_{i=0}^{n-1} \sum_{j=0}^{n-1} Z_{ij}^2 \quad (11)$$

This characteristic ensures preservation of the total image energy following transformation. Thus, an image or signal function  $I(t)$  may be approximated through a linear expansion of orthogonal polynomial basis functions as visualised in equation (12).

$$I(t) = \sum_{1 \leq i \leq p} \alpha_i u_{i-1}(t) \quad (12)$$

The coefficients are determined by the least squares method as represented in equation (13):

$$\alpha_i = \frac{\sum_{1 \leq t \leq n} I(t) u_i(t)}{\sum_{1 \leq t \leq n} u_i^2(t)} \quad (13)$$

The orthogonal polynomial basis operators corresponding to the  $(2 \times 2)$  dimensional case are defined as follows:

$$O_{00}^2 = \begin{bmatrix} 1 & 1 \\ 1 & 1 \end{bmatrix}, \quad O_{01}^2 = \begin{bmatrix} -1 & 1 \\ -1 & 1 \end{bmatrix}, \quad O_{10}^2 = \begin{bmatrix} -1 & -1 \\ 1 & 1 \end{bmatrix}$$

The orthogonal polynomial basis operators corresponding to the  $(3 \times 3)$  dimensional case are defined as follows:

$$O_{00}^3 = \begin{bmatrix} 1 & 1 & 1 \\ 1 & 1 & 1 \\ 1 & 1 & 1 \end{bmatrix}, \quad O_{01}^3 = \begin{bmatrix} -1 & 0 & 1 \\ -1 & 0 & 1 \\ -1 & 0 & 1 \end{bmatrix},$$

$$O_{10}^3 = \begin{bmatrix} -1 & -1 & -1 \\ 0 & 0 & 0 \\ 1 & 1 & 1 \end{bmatrix}, \quad O_{11}^3 = \begin{bmatrix} 1 & 0 & -1 \\ 0 & 0 & 0 \\ -1 & 0 & 1 \end{bmatrix},$$

$$O_{20}^3 = \begin{bmatrix} 1 & 1 & 1 \\ -2 & -2 & -2 \\ 1 & 1 & 1 \end{bmatrix}, \quad O_{21}^3 = \begin{bmatrix} 1 & 0 & 1 \\ 2 & 0 & -2 \\ -1 & 0 & 1 \end{bmatrix},$$

The polynomial operators defined over the  $(n \times n)$  dimensions, where  $n \geq 2$ , forms a complete orthogonal basis whose elements are linearly independent.

### 2.3 Quantum-Inspired Qubit Extraction Method

Quantum-inspired learning frameworks map classical medical image features into quantum state representations to exploit principles such as superposition, rotation-based encoding, and inter-feature correlation modeling in a high-dimensional Hilbert space. A qubit is described as a superposition of the computational basis states, written as their linear combination as shown in equation (14).

$$|\psi\rangle = \alpha|0\rangle + \beta|1\rangle, \quad \text{where } |\alpha|^2 + |\beta|^2 = 1, \quad (14)$$

ensuring valid probability amplitudes.

In brain tumor MRI analysis, enhanced tumor-related features such as edges, textures, and deep representations are first normalized and then encoded into quantum-inspired states. Given a classical feature vector  $\mathbf{x} = [x_1, x_2, \dots, x_d]$ , the corresponding Hilbert space encoding is defined as described in equation (15).

$$|\psi\rangle = \sum_{i=1}^d \tilde{x}_i |i\rangle, \quad \tilde{x}_i = \frac{x_i}{\|\mathbf{x}\|}. \quad (15)$$

This superposition-based representation enables simultaneous modeling of multiple tumor characteristics.

To parameterize the feature-to-qubit transformation, each enhanced feature is encoded using rotation-based quantum-inspired gates as depicted in equation (16).

$$|\psi_{ij}\rangle = R_z(\theta_{ij}) R_y(\phi_{ij}) |0\rangle, \quad (16)$$

where  $\theta_{ij}$  and  $\phi_{ij}$  are rotation angles derived from tumor-specific feature values. This encoding allows continuous MRI features to be efficiently mapped into qubit-like states.

To model inter-feature dependencies, entanglement-inspired correlations are introduced through controlled rotation mechanisms. The correlation between two encoded feature states is extracted as represented in equation (17).

$$F_{ij} = \langle Z_i \otimes Z_j \rangle, \quad (17)$$

which is conceptually analogous to the application of an  $RZZ(\theta)$  gate in quantum systems. This formulation enables correlated tumor patterns to be jointly represented.

Finally, similarity between two encoded MRI samples is computed using a quantum-inspired kernel defined as described in equation (18).

$$K(\psi_i, \psi_j) = |\langle \psi_i | \psi_j \rangle|^2, \quad (18)$$

which facilitates nonlinear separation in the induced Hilbert space and forms the theoretical basis for the QSVM used in brain tumor classification.

## 3 Literature Review

The CNN model developed by Sharma et al. (2025) is used to diagnose and identify brain tumours on MRI images. They are a feature-learner of spatial features, which is automatic and induces greater accuracy in comparison with conventional handcrafted features techniques [1]. It can also do end to end learning with minimal preprocessing. The architecture however

is represented in a classical Euclidean feature space, and no longer models explicitly a complex nonlinear interaction of features and edge effects, which may be less useful where tumor boundaries are diffuse.

As Solaiman and Solaiman (2025) have dubbed it as a multi-class transfer learning approach, brain tumors classification is based on a fully trained deep neural network[2]. It results in high features extraction, high-speed training and high generalization with small medical datasets through optimizing the large pre-trained models. Nevertheless, excessive application of pretrained structures might result in a reduced ability to adjust to tumor specificities and the inability to implement features and improve limits can have an impact on resilience in the situations when the tumors are woven.

DeepResNet, which is a residual transfer learning model, proposed by A. R. S. L, et al. (2025), and it was designed for the detection of brain tumors[5]. The model is convergence-stable and improves the results of detection through the incorporation of deep residual connections and pretrained networks. However, it is still in the common deep learning framework, and lacks high-level feature combination, quantum-inspired designs, and explicit texture and edge-enhancements that are essential in the complex tumor morphologies.

The model of transfer learning was developed by Srivastava (2025). in a hybrid classical-quantum model, and a quantum neural network was applied in classifying brain tumors[6]. The mixture will improve the results of feature representation and classification. However, the structure does not incorporate any direct edge or texture enhancement and does not have clearly established plan of quantum feature fusion. Specific flexibility of data sets may also be restrictive in the process of transfer learning.

Chen et al. (2018) came up with the concept of a deep architecture, also referred to as DRI-Net, which has density connections, residual learning, and initializing modules to segment medical images[4]. The model works well in contextual multi-scale information and also it is highly beneficial as regards to better feature reuse and gradient stability. It is computationally costly but, first of all, designed to partition and not to classify, and live in a classical feature representation space.

Akpinar et al. (2025) suggested a quantum-enhanced model, which was based on the fact that the brain tumors would be detected by the presence of the genes of the DNA microarray[7]. Through quantum computing, the strategy investigates the nonlinear dynamics of the high-dimensional genomic properties and enhances the prediction. The article however does not take into account the space tumor characteristics but the genomic information as compared to MRI imaging. In addition to it, its clinical use is limited to the necessity to have particular quantum computing facilities.

## **4 The Proposed QuAntNet Method**

The proposed QuAntNet system adopts a hybrid classical-quantum inspired design to enable accurate brain tumor detection and multi-category classification from MRI images. As shown in the Figure 1, the framework is structured into two main phases: Classical Feature Extraction (CFE) and the Quantum Image Diagnosis Engine(QIDE). The procedure starts with training and testing of MRI scans, then edges, textures and deep feature detection pointing out important structural information like the boundaries of tumors, changes in shape and texture. A polarization process is then used to boost high-frequency and reduce feature redundancy of the image that boosts tumor region separability[14].

After the preprocessing, discriminative feature extraction is carried out to extract spatial, intensity and structural features to be used in tumor analysis[3]. These characteristics are next sent to OPCNN-QFF method. This module is used to encode the classical features in

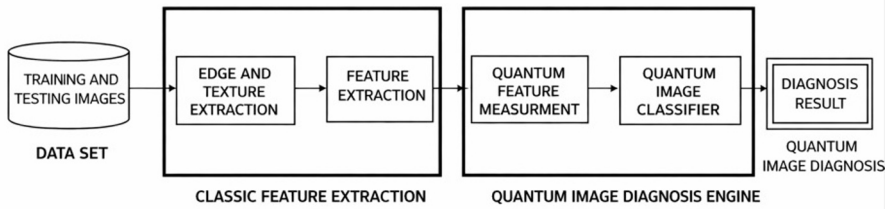


**Figure 1.** The Pipeline of the Proposed QuAntNet Method

quantum-inspired states and combine them with the principles of superposition and entanglement to model complicated feature relations.

Finally, the fused quantum-inspired representation is classified using a QSVM. Operating within a quantum-inspired Hilbert space, QSVM determines optimal decision boundaries to produce accurate tumor class predictions, delivering a robust diagnostic outcome.

#### 4.1 The Proposed OPCNN-QFF Method

The basic principles of quantum-inspired quantum groups on which qualitative Orthogonal Polynomials Based Quantum Feature Fusion(OPCNN-QFF) is based are superposition, probability amplification and entanglement, but does not rest on a quantum system but may be actually implemented on classical computing hardware. The fusion approach is to predict complex correlations of the deep features obtained based on the brain MRI images and generate a small discriminative expression that is highly accurate in obtaining the tumor classification.

Let the OPCNN-QFF backbone extract a set of edge, texture and deep feature vectors from the input MRI image as observed in equation (19):

$$F = \{f_1, f_2, \dots, f_N\}, \quad f_i \in \mathbb{R}^d \quad (19)$$

A quantum-inspired probability amplitude vector is created by normalizing each feature vector as described in equation (20):

$$\psi_i = \frac{f_i}{\|f_i\|} \quad (20)$$

where  $\psi_i$  is a quantum-inspired feature state that is comparable to a Hilbert space quantum state vector. The quantum probability constraint is enforced by the normalization as represented in equation (21):

$$\sum_{k=1}^d |\psi_{ik}|^2 = 1 \quad (21)$$

A unified feature representation is formed by linearly integrating multiple feature states, inspired by the quantum superposition principle as shown in equation (22).

$$|\Psi\rangle = \sum_{i=1}^N \alpha_i |\psi_i\rangle \quad (22)$$

Multiple discriminative properties can affect classification in this formulation, where  $|\psi_i\rangle$  indicates quantum-inspired feature states and  $\alpha_i$  represents their contribution weights within the

fused representation. An entanglement-based attention mechanism is used to further model feature interdependencies. The correlations between  $|\psi_i\rangle$  and  $|\psi_j\rangle$  are calculated by taking their inner product as illustrated in equation (23).

$$E_{ij} = \langle \psi_i | \psi_j \rangle \quad (23)$$

where  $E_{ij}$  quantifies the correlation strength between feature pairs as shown in equation (24).

$$A_{ij} = \frac{\exp(E_{ij})}{\sum_{j=1}^N \exp(E_{ij})} \quad (24)$$

The attention matrix depicts entanglement-like relationships which are devoted to highly correlated and informative state of features. The eventual fused representation is the weighted fused result of the resultant fused representation, which resembles quantum-inspired process of measurement as depicted in equation (25).

$$F_{\text{fused}} = \sum_{i=1}^N A_i \cdot \psi_i \quad (25)$$

To ensure numerical stability and compatibility with subsequent classification, the fused feature vector is normalized as described in equation (26):

$$\hat{F}_{\text{fused}} = \frac{F_{\text{fused}}}{\|F_{\text{fused}}\|} \quad (26)$$

Instead of a traditional fully connected layer, the normalized fused feature vector  $\hat{F}_{\text{fused}}$  is classified using a QSVM. This classifier aligns with the Hilbert space representation of the features and leverages inner-product kernel functions based on quantum similarity principles. The QSVM optimization objective is formulated as follows as described in equation (27)-(28):

$$\min_{\mathbf{w}, b} \frac{1}{2} \|\mathbf{w}\|^2 + C \sum_{i=1}^N \xi_i \quad (27)$$

Provided that:

$$y_i (\langle \mathbf{w}, \hat{F}_{\text{fused}}^{(i)} \rangle + b) \geq 1 - \xi_i \quad (28)$$

where  $\mathbf{w}$  and  $b$  are the learnable parameters,  $C$  is the regularization parameter,  $\xi_i$  are slack variables, and  $y_i$  denotes the tumor class labels.

The QSVM employs a quantum-inspired kernel based on the inner product between fused feature states as represented in equation (29):

$$K(\psi_i, \psi_j) = |\langle \psi_i | \psi_j \rangle|^2 \quad (29)$$

which effectively captures nonlinear decision boundaries and complex feature correlations within the quantum-inspired feature space. After obtaining the normalized fused quantum-inspired feature vector  $\hat{F}_{\text{fused}}$ , the QSVM computes the decision function as shown in equation (30):

$$f(x) = \sum_{i=1}^N \alpha_i y_i K(x, x_i) + b \quad (30)$$

In this expression,  $\alpha_i$  represent the optimized support vector weights,  $y_i$  correspond to the labels associated with the support vectors,  $K(\cdot, \cdot)$  refers to the quantum-inspired kernel, and  $b$  denotes the offset (bias) term.

For binary classification, the predicted class label is obtained as depicted in equation(31):

$$\hat{y} = \text{sign}(f(x)) \quad (31)$$

For multi-class tumor classification, a one-vs-rest strategy is employed, and the final predicted class is determined as in equation (32):

$$\hat{y} = \arg \max_k f_k(x) \quad (32)$$

In this case,  $f_k(x)$  is the decision function of each tumor category. QSVM is used as the last classification step which puts the fused quantum inspired features in the respective tumor category. It works in the Hilbert feature space which effectively represents nonlinear boundaries between decisions so that it correctly and effectively diagnoses brain tumors.

## 5 Experimental Results

### 5.1 Dataset Description

The BraTS 2020 dataset comprises 369 multi-modal brain MRI images with four various MRI modalities, which are T1, T1ce, T2, and FLAIR and expert-labeled tumors, which is used to classify the tumors into High Grade Glioma(HGG) and Low Grade Glioma(LGG)[15]. This dataset identifies visible tumor representative 2D slices to classify them and removes those that are not tumors to minimize redundancy and disequilibrium of classes. On the other hand, Figshare dataset, in which 3,064 T1-weighted contrast-enhanced MRI images are involved, enables multi-class tumor classification into four categories and the distribution of the classes in it is balanced, which enables us to assess the multi-class classification models adequately.

### 5.2 Performance Measures

To quantitatively assess the performance of the proposed approach QuAntNet framework combined with the OPCNN-QFF and QSVM classifier, several standard performance metrics are employed. These measures are described in equation (33)-(36).

$$\text{Accuracy} = \frac{TP + TN}{TP + TN + FP + FN} \quad (33)$$

$$\text{Precision} = \frac{TP}{TP + FP} \quad (34)$$

$$\text{Recall} = \frac{TP}{TP + FN} \quad (35)$$

$$\text{F1-score} = \frac{2 \times \text{Precision} \times \text{Recall}}{\text{Precision} + \text{Recall}} \quad (36)$$

The basic performance measure is the accuracy metric which reveals the overall correctness of the classification model. It is estimated as the proportion of the positively classified instances of the total amount of instances. Precision is reliability of the positive predictions, the estimation is the ratio between the true positive results and the total number of the instances that are classified as positive. Conversely, the sensitivity or the recall of the model is the capacity of the model to forecast the actual positive instances accurately.

### 5.3 Experiment on BraTS 2020 Dataset

To test the proposed quantum-inspired framework, the BraTS 2020 dataset is used to examine the efficiency of the framework in the tumor grade classification problem. It is made up of 369 multi-modal MRI scans of the brains 3D with T1, T1ce, T2, and FLAIR that are used to determine the distinction between the HGG and LGG types of tumors [15].

Out of the 3D volumes of MRI, relevant 2D axial slices are then obtained in which a clear tumor can be seen. The slices without a tumor are removed to get rid of redundancy and minimize the classes imbalance. The retained images are scaled to homogeneous resolution, and normalized in terms of intensity and then the features are extracted.

The proposed CFE method automatically extracts edge, texture and deep features based on OPT and CNN techniques, which is critical for distinguishing tumour grades. These features are transformed into quantum-inspired feature states and fused using the proposed OPCNN-QFF module, which models inter-feature dependencies through superposition and entanglement-inspired attention as shown in Table 1. For the BraTS 2020 dataset, which involves binary tumor grading between HGG and LGG, the proposed framework attains strong classification performance using a 10-qubit configuration. This relatively lower number of qubits is sufficient due to the application of the OPT, which enhances tumor boundaries and texture details while reducing feature redundancy prior to quantum encoding. Each refined feature vector is encoded into quantum-inspired states through single-qubit rotation operations, mainly using the  $R_y(\phi)$  and  $R_z(\theta)$  gates. These rotations encode intensity, edge, and texture features into quantum probability representations. The concept of multi-qubit entanglement is employed to simulate correlations among discriminative tumor phenotypes using Controlled-Z (CZ) gates or parameterized  $R_{ZZ}(\theta)$  gates.

The extracted expectation values are then provided to a QSVM, which determines the decision boundary in the quantum-inspired Hilbert space. The QSVM effectively classifies the fused feature representations and achieves high accuracy and sensitivity on the BraTS 2020 dataset. Additionally, edge-enhanced preprocessing along with the feature fusion process further improves the model's capability to handle complex medical imaging data.

### 5.4 Experiment on Figshare Dataset

The proposed framework is further validated on Figshare brain tumor MRI dataset for multi-class classification. The dataset contains 3,064 images distributed across four categories: glioma (826), meningioma (822), pituitary tumor (827), and no-tumor cases (619).

Resize all pictures to one common resolution and bring them into normalization so that there is consistency among the samples[13]. Edge and texture features will enhance tumor boundaries and structural patterns, then deep features are extracted using the backbone of OPT and CNN techniques.

Texture and deep features obtained are mapped into quantum-inspired feature states and fused (using the proposed OPCNN-QFF module). It makes use of the correlations existing between features at different levels so as to realize a compact dimension that will be very informative toward realizing multi-class classification. For the Figshare brain tumor MRI dataset, which involves multi-class classification across four tumor categories, namely glioma, meningioma, pituitary tumor, and normal tissue, a higher representational capacity is required due to increased class overlap and structural variability. Consequently, the proposed framework employs 12 qubits to encode the enhanced classical features. Similar to the BraTS 2020 setup, OPT is first applied to emphasize tumor edges and texture patterns, thereby improving class separability prior to quantum encoding.

Feature encoding is performed by single-qubit rotation gates, viz.,  $R_y(\phi)$  and  $R_z(\theta)$ , while multi-layer entanglement is introduced using CZ gates or parameterized  $R_{ZZ}(\theta)$  gates to capture complex inter-class relationships. Compared to the binary classification case, a denser entanglement structure is required to effectively model nonlinear decision boundaries among multiple tumor categories. After the quantum measurement, the expectation values obtained are categorized with the help of a multi-class QSVM applied by one vs rest. Such quantum-inspired setup greatly improves the feature discrimination among all the tumor classes, leading to high accuracy and strength in the classification of the Figshare dataset.

An ensemble of multi-class QSVM is used to classify the fused features to be in the 4 tumor categories. The nonlinear edges of the classes and coinciding distributions of features can be addressed effectively in the QSVM through the use of the kernel-based decision-making mechanism.

The experimental result using Figshare data shows that there is high classification performance on all the categories of tumor. The comparatively equal number of classes enables training and analysis to be steady, and the suggested quantum-inspired model presents great generalization performance in the multi-class brain tumor diagnosis as mentioned in Table 2.

## 5.5 Result and discussion

The proposed quantum-inspired brain tumor diagnosis framework is evaluated using the BraTS 2020 and Figshare MRI datasets. The results are benchmarked against two recent classical and one quantum baseline approaches: a CNN, DRI-Net and QNN models. Performance is evaluated using standard medical imaging metrics as shown in Table 1.

**Table 1.** Performance Evaluation of Various Methods on the BraTS 2020 Dataset

Method	Accuracy (%)	Sensitivity (%)	Specificity (%)	F1-score (%)
CNN	93.8	92.5	94.6	93.1
DRI-Net	95.4	94.2	96.1	94.8
QNN	96.5	95.9	97.1	96.2
<b>QuAntNet</b>	<b>98.7</b>	<b>98.2</b>	<b>99.0</b>	<b>98.4</b>

The CNN-based method achieves an accuracy of 93.8%, with sensitivity and specificity of 92.5% and 94.6%, respectively, indicating limited capability in capturing subtle structural differences between HGG and LGG using conventional feature extraction[11]. The DRI-Net-based approach improves performance to 95.4% accuracy and 96.1% specificity, benefiting from deeper residual feature learning; however, it remains constrained by classical feature space representations[4].

The QNN model upgraded classification performance, attaining 96.5% accuracy, 95.9% sensitivity, and 97.1% specificity since it can encode lesion features in a quantum-inspired Hilbert space making nonlinear relations better modeled than typical spaces. However, since there is not any explicit mechanism for inter-feature dependency modeling in this setup, it has an overall discriminative capability reflected by an F1-score of only 96.2%.

The proposed QuAntNet model outperforms all compared approaches, achieving an accuracy of 98.7%, sensitivity of 98.2%, specificity of 99.0%, and an F1-score of 98.4%. Feature redundancy reduction based on orthogonal polynomials for transformation theoretically enhances boundary and texture information toward sensitivity and quantum feature fusion leveraging superposition and entanglement-inspired attentions to capture correlated features characteristic of tumors provide a theoretical basis for the performance improvement claimed above. In addition, QSVM adds strength to classification by building a maximum-margin

decision boundary in a quantum-inspired feature space to ensure robustness that translates into generalization.

On the Figshare dataset result shown in Table 2, the CNN-based model has an accuracy rate of 94.6% with the sensitivity and specificity of 93.9% and 95.2%, respectively. The model is to a great extent capable of distinguishing between significant types of tumors, and its performance is not very high because of the overlapping features distributions between glioma, meningioma, pituitary tumor, and normal classes. Diagnosis accuracy rises to 96.1% when using the DRI-Net-based approach and Specificity up to 96.8% owing to deeper residual learning however stuck with classical feature representations[4].

The QNN model pushed metrics up to 97.4% overall accuracy, 96.9% sensitivity, and 98.0% specificity by encoding discriminative tumor features within the quantum-inspired Hilbert space representation, making visually similar classes more separable than what can be obtained through classical Hilbert spaces. However, since there is no explicit feature fusion mechanism available to help capture complex inter-class relationships fully, the best achievable F1-score value would be just around 97.2%.

QuAntNet achieves the best overall results across all evaluation metrics, recording an accuracy of 99.3%, sensitivity of 98.9%, specificity of 99.6%, and an F1-score of 99.1%. Thus, theoretically justified are enhancements brought about by orthogonal polynomial-based edge and texture enhancement on one hand for better explicit representation of tumor boundaries and quantum feature fusion that reveals higher-order dependencies among deep features on the other hand. QSVM classifier further enhances robustness in multi-class separation through margin maximization in a quantum-inspired feature space formulation to generalize well over all classes of tumors.

**Table 2.** Performance Evaluation of Various Methods on the Figshare Dataset

Method	Accuracy (%)	Sensitivity (%)	Specificity (%)	F1-score (%)
CNN	94.6	93.9	95.2	94.1
DRI-Net	96.1	95.6	96.8	95.9
QNN	97.4	96.9	98.0	97.2
<b>QuAntNet</b>	<b>99.3</b>	<b>98.9</b>	<b>99.6</b>	<b>99.1</b>

## 6 Conclusion and Future Enhancement

This improved quantum-based framework for the automated diagnosis of brain tumors is introduced here, based on QuAntNet. This enhanced model incorporates integral transformations made by orthogonal polynomials to facilitate enhancement features at the edge and texture levels and CNN based deep features integrates quantum feature fusion thereby modeling inter-feature dependencies, and finally applies classification with a QSVM. Superposition, entanglement, and Hilbert space-based representation from quantum-inspired principles are leveraged to comprehensively gather both fine local discriminative features as well as global contextual relationships from MRI images of brains. The proposed system performed better on both BraTS 2020 and Figshare datasets than the standard CNN-based systems, DRI-Net-based systems, and standalone QNN models with respect to accuracy in binary and multi-classifications according to sensitivity, specificity, and F1-scores of 98.4% and 99.1% for BraTS 2020 and Figshare datasets respectively. The findings indicate the validity and versatility of the suggested methodology to complicated medical images. In the future, the extensions of this framework to take advantage of three-dimensional volumetric MRI data

and multi-modal fusion, with the aim of improving spatial context modeling, could be improved. The other field that can be explored involves executing the suggested model on hybrid quantum classical or emerging quantum computing systems in a manner that exploits real quantum computational advantages.

## References

- [1] A. Sharma, A. Pal, M. Gupta, Image classification and detection of brain tumor. Proc. 3rd Int. Conf. Communication, Security, and Artificial Intelligence (ICCSAI)1357–1361 (2025). <https://doi.org/10.1109/ICCSAI64074.2025.11064665>
- [2] F. Solaiman, M. Solaiman, Beneath the skull: Leveraging transfer learning for multi-class brain tumor classification. Proc. Interdisciplinary Conf. Electrics and Computer (INTCEC) 1–6 (2025). <https://doi.org/10.1109/INTCEC65580.2025.11255997>
- [3] S. Pereira, A. Pinto, V. Alves, C. A. Silva, Brain tumor segmentation using convolutional neural networks in MRI images. IEEE Trans. Med. Imaging 35, 1240–1251 (2016). <https://doi.org/10.1109/TMI.2016.2538465>
- [4] L. Chen, P. Bentley, K. Mori, K. Misawa, M. Fujiwara, D. Rueckert, DRINet for medical image segmentation. IEEE Trans. Med. Imaging 37, 2453–2462 (2018). <https://doi.org/10.1109/TMI.2018.2835303>
- [5] A. R. S. L., S. Yerram, N. Rajender, S. S. Rekha, S. K., K. S. Prasad, DeepResNet: A residual deep transfer model for enhanced brain tumor detection in MRI scans. Proc. Int. Conf. Information, Implementation, and Innovation in Technology (I2ITCON) 1–6 (2025). <https://doi.org/10.1109/I2ITCON65200.2025.11210738>
- [6] A. K. Srivastava, S. Sharma, S. Hussain, S. Ghosh, N. Sharma, A hybrid classical-quantum model for enhanced MRI-based brain tumor classification using transfer learning and quantum neural networks. Proc. 3rd Int. Conf. Communication, Security, and Artificial Intelligence (ICCSAI) 225–230 (2025). <https://doi.org/10.1109/ICCSAI64074.2025.11064720>
- [7] E. Akpınar, B. Hangun, M. Oduncuoglu, O. Altun, O. Eyecioglu, Z. Yalcin, Quantum-enhanced classification of brain tumors using DNA microarray gene expression profiles. Proc. IEEE Computer Society Annual Symposium on VLSI (ISVLSI) 1–6 (2025). <https://doi.org/10.1109/ISVLSI65124.2025.11130207>
- [8] A. J., V. S. Kumari, Hybrid red piranha optimization and quantum boosting for brain tumor classification. Proc. Int. Conf. Cognitive Robotics and Intelligent Systems (ICC-ROBINS) 1–6 (2025). <https://doi.org/10.1109/ICC-ROBINS64345.2025.11086158>
- [9] M. A. Islam, S. M. S. K. Talib, A. A. Noman, M. J. Hoque, M. I. K. Sakur, A. M. Chowdhury, A hybrid Res-BRNet architecture for efficient and accurate brain tumor classification. Proc. Int. Conf. Quantum Photonics, Artificial Intelligence, and Networking (QPAIN) 1–6 (2025). <https://doi.org/10.1109/QPAIN66474.2025.11171801>
- [10] G. Mounika, S. Kollem, S. Samala, Enhanced feature fused vision transformer framework for multiclass brain tumor classification using MRI images. Proc. Int. Conf. Innovations in Intelligent Systems: Advancements in Computing, Communication, and Cybersecurity (ISAC3) 1–6 (2025). <https://doi.org/10.1109/ISAC364032.2025.11156724>
- [11] X. Zhang, A highly accurate attention-based convolutional neural network for classification of brain tumors. Proc. Int. Conf. Computer Vision, Image and Deep Learning & Computer Engineering Applications (CVIDL & ICCEA) 124–128 (2022). <https://doi.org/10.1109/CVIDLICCEA56201.2022.9825036>
- [12] A. Taher, S. Anan, Multiclass brain tumor classification and segmentation from 2D MR images using custom CNN and residual attention U-Net.

- Proc. Int. Conf. Computer and Information Technology (ICCIT) 1–6 (2023).  
<https://doi.org/10.1109/ICCIT60459.2023.10441606>
- [13] R. Khan, R. Islam, Robust multiclass brain tumor classification using Swin transformer and feature optimization with ensemble learning. Proc. Int. Conf. Electrical, Computer and Communication Engineering (ECCE) 1–6 (2025).  
<https://doi.org/10.1109/ECCE64574.2025.11013470>
- [14] R. Krishnamoorthi, N. Kannan, A new integer image coding technique based on orthogonal polynomials. Image Vis. Comput. 27, 999–1006 (2009).  
<https://doi.org/10.1016/j.imavis.2008.08.006>
- [15] B. H. Menze et al., The multimodal brain tumor image segmentation benchmark (BRATS).IEEE Trans. Med. Imaging 34, 1993–2024 (2015).  
<https://doi.org/10.1109/TMI.2014.2377694>